

# Polyakov loop extended NJL model with imaginary chemical potential

Yuji Sakai,<sup>1,\*</sup> Kouji Kashiwa,<sup>1,†</sup> Hiroaki Kouno,<sup>2,‡</sup> and Masanobu Yahiro<sup>1,§</sup>

<sup>1</sup>*Department of Physics, Graduate School of Sciences, Kyushu University, Fukuoka 812-8581, Japan*

<sup>2</sup>*Department of Physics, Saga University, Saga 840-8502, Japan*

(Dated: February 2, 2008)

The Polyakov loop extended Nambu–Jona-Lasinio (PNJL) model with imaginary chemical potential is studied. The model possesses the extended  $\mathbb{Z}_3$  symmetry that QCD does. Quantities invariant under the extended  $\mathbb{Z}_3$  symmetry, such as the partition function, the chiral condensate and the modified Polyakov loop, have the Roberge-Weiss (RW) periodicity. The phase diagram of confinement/deconfinement transition derived with the PNJL model is consistent with the RW prediction on it and the results of lattice QCD. The phase diagram of chiral transition is also presented by the PNJL model.

PACS numbers: 11.30.Rd, 12.40.-y

With the aid of the progress in computer power, lattice QCD simulations have become feasible for thermal systems at zero quark chemical potential ( $\mu$ ) [1]. As for  $\mu > 0$ , however, lattice QCD has the well-known sign problem, and then the results are still far from perfection; for example, see Ref. [2] and references therein.

Several approaches have been proposed to solve the sign problem. One of them is the use of imaginary chemical potential, since the fermionic determinant that appears in the euclidean partition function is real in the case; for example, see Refs. [3, 4, 5, 6, 7, 8] and references therein. If the physical quantity such as chiral condensate is known in the imaginary  $\mu$  region, one can extrapolate it to the real  $\mu$  region, until there appears a discontinuity. Furthermore, in principle, one can evaluate with the Fourier transformation the canonical partition function with fixed quark number from the grand canonical partition function with imaginary chemical potential [9].

Roberge and Weiss (RW) [9] found that the partition function of  $SU(N)$  gauge theory with imaginary chemical potential  $\mu = i\theta/\beta$ ,

$$Z(\theta) = \int D\psi D\bar{\psi} D A_\mu \exp \left[ - \int d^4x \left\{ \bar{\psi}(\gamma D - m_0)\psi - \frac{1}{4} F_{\mu\nu}^2 - i \frac{\theta}{\beta} \bar{\psi} \gamma_4 \psi \right\} \right], \quad (1)$$

is a periodic function of  $\theta$  with a period  $2\pi/N$ , that is  $Z(\theta + 2\pi k/N) = Z(\theta)$  for any integer  $k$ , by showing that  $Z(\theta + 2\pi k/N)$  is reduced to  $Z(\theta)$  with the  $\mathbb{Z}_N$  transformation

$$\psi \rightarrow U\psi, \quad A_\nu \rightarrow U A_\nu U^{-1} - \frac{i}{g} (\partial_\nu U) U^{-1}, \quad (2)$$

where  $U(x, \tau)$  are elements of  $SU(N)$  with the boundary condition  $U(x, \beta) = \exp(-2i\pi k/N)U(x, 0)$ . Here  $\psi$  is the fermion field with mass  $m_0$ ,  $F_{\mu\nu}$  is the strength tensor of the gauge field  $A_\mu$ , and  $\beta$  is the inverse of temperature  $T$ . The RW

periodicity means that  $Z(\theta)$  is invariant under the extended  $\mathbb{Z}_N$  transformation

$$\theta \rightarrow \theta + \frac{2\pi k}{N}, \quad \psi \rightarrow U\psi, \quad A_\nu \rightarrow U A_\nu U^{-1} - \frac{i}{g} (\partial_\nu U) U^{-1}. \quad (3)$$

Quantities invariant under the extended  $\mathbb{Z}_N$  transformation, such as the thermodynamic potential  $\Omega(\theta)$  and the chiral condensate, keep the RW periodicity. Meanwhile, the Polyakov loop  $\Phi$  is not invariant under the transformation (3), since it is transformed as  $\Phi \rightarrow \Phi e^{-i2\pi k/N}$ . In general, non-invariant quantities such as  $\Phi$  do not have the periodicity. Roberge and Weiss also showed with perturbation that in the high  $T$  region  $d\Omega(\theta)/d\theta$  and  $\Phi$  are discontinuous as a function of  $\theta$  at values of  $(2k+1)\pi/N$ , and also found with the strong coupled lattice theory that the discontinuities disappear in the low  $T$  region. This is called the Roberge-Weiss phase transition of first order, and is observed in lattice simulations [3, 4, 5, 6, 7, 8].

Figure 1 shows a predicted phase diagram in the  $\theta$ - $T$  plane. The solid lines represent the RW discontinuities of the Polyakov loop, and the dot-dashed lines do the chiral phase transition predicted by the lattice simulations, although results of the simulations are not conclusive yet since it is hard to take the chiral limit in the simulations. In this paper, the term “chiral phase transition” (“deconfinement phase transition”) is used whenever the chiral condensate (the Polyakov loop) is discontinuous or not smooth.

As an approach complementary to first-principle lattice simulations, one can consider several effective models. One of them is the Nambu–Jona-Lasinio (NJL) model [10]. Although the NJL model is a useful method for understanding the chiral symmetry breaking, this model does not possess a confinement mechanism. As a reliable model that can treat both the chiral and the deconfinement phase transition, we can consider the Polyakov loop extended NJL (PNJL) model [11, 12, 13, 14, 15, 16, 17, 18, 19, 20]. In the PNJL model the deconfinement phase transition is described by the Polyakov loop. It is known that effects of the Polyakov loop make the critical endpoint [21, 22, 23, 24] move to higher  $T$  and lower  $\mu$  than the NJL model predicts [17, 20].

The PNJL model has the extended  $\mathbb{Z}_3$  symmetry needed to reproduce the RW periodicity, as shown later. In this paper, we study the phase diagram in the  $\theta$ - $T$  plane by using the PNJL model. Both the chiral and the deconfinement phase

\*sakai2scp@mbox.nc.kyushu-u.ac.jp

†kashiwa2scp@mbox.nc.kyushu-u.ac.jp

‡kounoh@cc.saga-u.ac.jp

§yahiro2scp@mbox.nc.kyushu-u.ac.jp

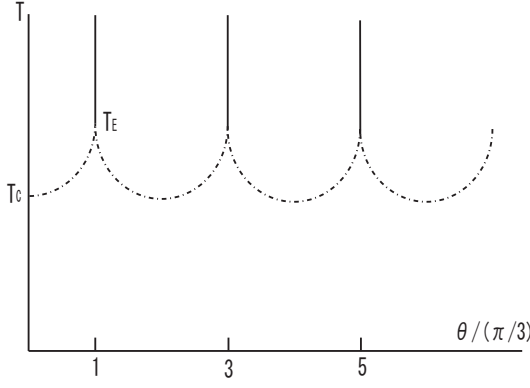


Fig. 1: The RW prediction on the QCD phase diagram in the  $\theta - T$  plane. The solid lines represent the confinement/deconfinement phase transition of first order, and the dot-dashed ones correspond to the chiral phase transition of second order.

transition are analyzed in the chiral ( $m_0 = 0$ ) limit where the lattice simulation is not available.

The model we consider is the following two-flavor PNJL Lagrangian,

$$\mathcal{L} = \bar{q}(i\gamma_\nu D^\nu - m_0)q + G_s[(\bar{q}q)^2 + (\bar{q}i\gamma_5 \vec{\tau}q)^2] - \mathcal{U}(\Phi[A], \Phi[A]^*, T), \quad (4)$$

where  $q$  denotes the two-flavor quark field,  $m_0$  does the current quark mass, and  $D^\nu = \partial^\nu - iA^\nu + \delta_0^\nu \mu$  for the chemical potential  $\mu = i\theta/\beta$ . The field  $A^\nu$  is defined as  $A^\nu = \delta_{\nu 0} g A_a^\nu \frac{\lambda_a}{2}$  with the gauge field  $A_a^\nu$ , the Gell-Mann matrix  $\lambda_a$  and the gauge coupling  $g$ . In the NJL sector,  $\vec{\tau}$  stands for the isospin matrix, and  $G_s$  denotes the coupling constant of the scalar type four-quark interaction. The Polyakov potential  $\mathcal{U}$ , defined later in (11), is a function of the Polyakov loop  $\Phi$  and its complex conjugate  $\Phi^*$ ,

$$\Phi = \frac{1}{N_c} \text{Tr} L, \quad \Phi^* = \frac{1}{N_c} \text{Tr} L^\dagger, \quad (5)$$

with

$$L(\mathbf{x}) = \mathcal{P} \exp \left[ i \int_0^\beta d\tau A_4(\mathbf{x}, \tau) \right], \quad (6)$$

where  $\mathcal{P}$  is the path ordering,  $A_4 = iA_0$  and  $N_c = 3$ . In the chiral limit ( $m_0 = 0$ ), the Lagrangian density has the exact  $SU(2)_L \times SU(2)_R \times U(1)_v \times SU(3)_c$  symmetry.

The temporal component  $A_4$  is diagonal in the flavor space, because the color and the flavor space are completely separated out in the present case. In the Polyakov gauge,  $L$  can be written in a diagonal form in the color space [12]:

$$L = e^{i\beta(\phi_3 \lambda_3 + \phi_8 \lambda_8)} = \text{diag}(e^{i\beta\phi_a}, e^{i\beta\phi_b}, e^{i\beta\phi_c}), \quad (7)$$

where  $\phi_a = \phi_3 + \phi_8/\sqrt{3}$ ,  $\phi_b = -\phi_3 + \phi_8/\sqrt{3}$  and  $\phi_c = -(\phi_a + \phi_b) = -2\phi_8/\sqrt{3}$ . The Polyakov loop  $\Phi$  is an exact order parameter of the spontaneous  $\mathbb{Z}_3$  symmetry breaking in

the pure gauge theory. Although the  $\mathbb{Z}_3$  symmetry is not exact in the system with dynamical quarks, it still seems to be a good indicator of the deconfinement phase transition as discussed later. Therefore, we use  $\Phi$  to define the deconfinement phase transition.

Under the mean field approximation (MFA), the Lagrangian density becomes

$$\mathcal{L}_{\text{MFA}} = \bar{q}(i\gamma_\mu D^\mu - (m_0 + \Sigma_s))q - U(\sigma) - \mathcal{U}(\Phi, \Phi^*, T), \quad (8)$$

where

$$\sigma = \langle \bar{q}q \rangle, \quad \Sigma_s = -2G_s \sigma, \quad U = G_s \sigma^2. \quad (9)$$

Using the usual techniques, one can obtain the thermodynamic potential

$$\begin{aligned} \Omega = & -2N_f V \int \frac{d^3 p}{(2\pi)^3} \left[ 3E(\mathbf{p}) \right. \\ & + \frac{1}{\beta} \ln [1 + 3(\Phi + \Phi^* e^{-\beta E^-(\mathbf{p})}) e^{-\beta E^-(\mathbf{p})} + e^{-3\beta E^-(\mathbf{p})}] \\ & + \frac{1}{\beta} \ln [1 + 3(\Phi^* + \Phi e^{-\beta E^+(\mathbf{p})}) e^{-\beta E^+(\mathbf{p})} + e^{-3\beta E^+(\mathbf{p})}] \left. \right] \\ & + (U + \mathcal{U})V, \end{aligned} \quad (10)$$

where  $E(\mathbf{p}) = \sqrt{\mathbf{p}^2 + M^2}$ ,  $E^\pm(\mathbf{p}) = E(\mathbf{p}) \pm i\theta/\beta$  and  $M = m_0 + \Sigma_s$ . We use  $\mathcal{U}$  of Ref. [15] that is fitted to the result of lattice simulation in the pure gauge theory at finite  $T$  [25, 26]:

$$\frac{\mathcal{U}}{T^4} = -\frac{b_2(T)}{2} \Phi^* \Phi - \frac{b_3}{6} (\Phi^{*3} + \Phi^3) + \frac{b_4}{4} (\Phi^* \Phi)^2, \quad (11)$$

$$b_2(T) = a_0 + a_1 \left( \frac{T_0}{T} \right) + a_2 \left( \frac{T_0}{T} \right)^2 + a_3 \left( \frac{T_0}{T} \right)^3, \quad (12)$$

where parameters are summarized in Table I. The Polyakov potential yields a deconfinement phase transition at  $T = T_0$  in the pure gauge theory. Hence,  $T_0$  is taken to be 270 MeV predicted by the pure gauge lattice QCD calculation.

$a_0$	$a_1$	$a_2$	$a_3$	$b_3$	$b_4$
6.75	-1.95	2.625	-7.44	0.75	7.5

TABLE I: Summary of the parameter set in the Polyakov sector used in Ref. [15]. All parameters are dimensionless.

The variables of  $\Phi$ ,  $\Phi^*$  and  $\sigma$  satisfy the stationary conditions,

$$\partial\Omega/\partial\Phi = 0, \quad \partial\Omega/\partial\Phi^* = 0, \quad \partial\Omega/\partial\sigma = 0. \quad (13)$$

The thermodynamic potential  $\Omega(\theta)$  at each  $\theta$  is obtained by inserting the solutions,  $\Phi(\theta)$ ,  $\Phi(\theta)^*$  and  $\sigma(\theta)$ , of (13) at each  $\theta$  into (10).

The thermodynamic potential  $\Omega$  is not invariant under the  $\mathbb{Z}_3$  transformation,  $\Phi(\theta) \rightarrow \Phi(\theta)e^{-i2\pi k/3}$  and  $\Phi(\theta)^* \rightarrow \Phi(\theta)^* e^{i2\pi k/3}$ , although  $\mathcal{U}$  of (11) is invariant. Instead of the

$\mathbb{Z}_3$  symmetry, however,  $\Omega$  is invariant under the extended  $\mathbb{Z}_3$  transformation,

$$\begin{aligned} e^{\pm i\theta} &\rightarrow e^{\pm i\theta} e^{\pm i\frac{2\pi k}{3}}, & \Phi(\theta) &\rightarrow \Phi(\theta) e^{-i\frac{2\pi k}{3}}, \\ \Phi(\theta)^* &\rightarrow \Phi(\theta)^* e^{i\frac{2\pi k}{3}}. \end{aligned} \quad (14)$$

---

The extended  $\mathbb{Z}_3$  transformation is then rewritten into

$$e^{\pm i\theta} \rightarrow e^{\pm i\theta} e^{\pm i\frac{2\pi k}{3}}, \quad \Psi(\theta) \rightarrow \Psi(\theta), \quad \Psi(\theta)^* \rightarrow \Psi(\theta)^*, \quad (15)$$

and  $\Omega$  is also into

$$\begin{aligned} \Omega = -2N_f V \int \frac{d^3 p}{(2\pi)^3} &\left[ 3E(\mathbf{p}) + \frac{1}{\beta} \ln [1 + 3\Psi e^{-\beta E(\mathbf{p})} + 3\Psi^* e^{-2\beta E(\mathbf{p})} e^{\beta\mu_B} + e^{-3\beta E(\mathbf{p})} e^{\beta\mu_B}] \right. \\ &+ \frac{1}{\beta} \ln [1 + 3\Psi^* e^{-\beta E(\mathbf{p})} + 3\Psi e^{-2\beta E(\mathbf{p})} e^{-\beta\mu_B} + e^{-3\beta E(\mathbf{p})} e^{-\beta\mu_B}] \Big] + UV \\ &+ \left[ -\frac{b_2(T)T^4}{2} \Psi^* \Psi - \frac{\beta_3(T)T^4}{6} (\Psi^*{}^3 e^{\beta\mu_B} + \Psi^3 e^{-\beta\mu_B}) + \frac{b_4 T^4}{4} (\Psi^* \Psi)^2 \right] V, \end{aligned} \quad (16)$$


---

where  $\mu_B = 3\mu = i3\theta/\beta$  is the baryonic chemical potential and the factor  $e^{\pm\beta\mu_B}$  is invariant under the transformation (15). Obviously,  $\Omega$  is invariant under the transformation (15).

Under the transformation  $\theta \rightarrow \theta + 2\pi k/3$ , (16) keeps the same form, if  $\Psi(\theta)$  and  $\Psi(\theta)^*$  are replaced by  $\Psi(\theta + 2\pi k/3)$  and  $\Psi(\theta + 2\pi k/3)^*$ , respectively. This means that the stationary conditions for  $\Psi(\theta)$  and  $\Psi(\theta)^*$  agree with those for  $\Psi(\theta + 2\pi k/3)$  and  $\Psi(\theta + 2\pi k/3)^*$ , respectively, and then that

$$\Psi(\theta + \frac{2\pi k}{3}) = \Psi(\theta) \quad \text{and} \quad \Psi(\theta + \frac{2\pi k}{3})^* = \Psi(\theta)^*. \quad (17)$$

The potential  $\Omega$  depends on  $\theta$  through  $\Psi(\theta)$ ,  $\Psi(\theta)^*$ ,  $\sigma(\theta)$  and  $e^{i\theta}$ . We then denote  $\Omega(\theta)$  by  $\Omega(\theta) = \Omega(\Psi(\theta), \Psi(\theta)^*, e^{i\theta})$ , where  $\sigma(\theta)$  is suppressed since it is irrelevant to proofs below. The RW periodicity of  $\Omega$  is then shown as

$$\begin{aligned} \Omega(\theta + \frac{2\pi k}{3}) &= \Omega(\Psi(\theta), \Psi(\theta)^*, e^{i\frac{2\pi k}{3} + i\theta}) \\ &= \Omega(\Psi(\theta), \Psi(\theta)^*, e^{i\theta}) = \Omega(\theta), \end{aligned} \quad (18)$$

by using (17) in the first equality and the extended  $\mathbb{Z}_3$  symmetry of  $\Omega$  in the second equality.

Equation (16) keeps the same form under the transformation  $\theta \rightarrow -\theta$ , if  $\Psi(\theta)$  and  $\Psi(\theta)^*$  are replaced by  $\Psi(-\theta)^*$  and  $\Psi(-\theta)$ , respectively. This indicates that

$$\Psi(-\theta) = \Psi(\theta)^* \quad \text{and} \quad \Psi(-\theta)^* = \Psi(\theta). \quad (19)$$

Furthermore,  $\Omega$  is a real function, as shown in (16). Using these properties, one can show that

$$\begin{aligned} \Omega(\theta) &= (\Omega(\theta))^* = \Omega(\Psi(\theta)^*, \Psi(\theta), e^{-i\theta}) \\ &= \Omega(\Psi(-\theta), \Psi(-\theta)^*, e^{-i\theta}) = \Omega(-\theta). \end{aligned} \quad (20)$$

Thus,  $\Omega$  is a periodic even function of  $\theta$  with a period  $2\pi/3$ . The chiral condensate  $\sigma(\theta)$  is also a periodic even function of

It is convenient to introduce new variables  $\Psi \equiv e^{i\theta}\Phi$  and  $\Psi^* \equiv e^{-i\theta}\Phi^*$  invariant under the transformation (14).

$\theta$ ,  $\sigma(\theta) = \sigma(\theta + 2\pi k/3) = \sigma(-\theta)$ , because it is given by  $\sigma(\theta) = d\Omega(\theta)/dm_0$ .

The modified Polyakov loop  $\Psi$  has a periodicity of (17). The real (imaginary) part of  $\Psi$  is even (odd) under the interchange  $\theta \leftrightarrow -\theta$ , because of (19):  $\text{Re}[\Psi(\theta)] = (\Psi(\theta) + \Psi(\theta)^*)/2 = \text{Re}[\Psi(-\theta)]$  and  $\text{Im}[\Psi(\theta)] = (\Psi(\theta) - \Psi(\theta)^*)/(2i) = -\text{Im}[\Psi(-\theta)]$ . Thus, the real (imaginary) part of  $\Psi$  is a periodic even (odd) function of  $\theta$ .

Since  $\Omega(\theta)$ ,  $\Psi(\theta)$  and  $\sigma(\theta)$  are periodic functions of  $\theta$  with a period  $2\pi/3$ , here we think a period  $0 \leq \theta \leq 2\pi/3$ . In the region, periodic even functions such as  $\Omega(\theta)$ ,  $\sigma(\theta)$  and  $\text{Re}[\Psi(\theta)]$  are symmetric with respect to a line  $\theta = \pi/3$ . This indicates that such an even function has a cusp at  $\theta = \pi/3$ , if the gradient  $\lim_{\theta \rightarrow \pi/3 \pm 0} d\Omega/d\theta$  is neither zero or infinity. Such a cusp comes out in the high  $T$  region, as shown later with numerical calculations. This means that the chiral phase transition at  $\theta = \pi/3$  is the second order.

Meanwhile,  $\text{Im}[\Psi(\theta)]$  is a periodic odd function, so that  $\text{Im}[\Psi(\pi/3 - \epsilon)] = -\text{Im}[\Psi(-\pi/3 + \epsilon)] = -\text{Im}[\Psi(\pi/3 + \epsilon)]$  for positive infinitesimal  $\epsilon$ . This indicates that  $\text{Im}[\Psi(\theta)]$  is discontinuous at  $\theta = \pi/3$ , if it is not naught there. This is precisely the RW phase transition, and seen in the high  $T$  region, as shown later. The deconfinement phase transition at  $\theta = \pi/3$  is the first order transition appearing in the imaginary part of  $\Psi$ .

When  $\Psi = \Psi^* = 0$ ,  $\Omega$  with  $T$  fixed depends only on the baryon number chemical potential  $\mu_B$ , and then not on the quark number chemical potential  $\mu$  explicitly. In this sense, quarks are “confined” in the PNJL model. Meanwhile, for the case of finite  $\Psi$ ,  $\Omega$  depends on both  $\mu_B$  and  $\mu$ , indicating that the system is in a mixed phase of baryons and quarks. Thus, the quark confinement is described by the PNJL model through the percentage of  $\mu_B$  and  $\mu$ , and the order parameter  $\Psi$  of the  $\mathbb{Z}_3$  symmetry is found to play an pseudo order parameter of the confinement transition practically.

Since the NJL model is nonrenormalizable, it is then needed to introduce a cutoff in the momentum integration. Here we take the three-dimensional momentum cutoff

$$\int \frac{d^3\mathbf{p}}{(2\pi)^3} \rightarrow \frac{1}{2\pi^2} \int_0^\Lambda dp p^2. \quad (21)$$

Hence, the present model has three parameters  $m_0$ ,  $\Lambda$ ,  $G_s$  in the NJL sector. Following Ref. [23], we take  $\Lambda = 0.6315$  GeV and  $G_s = 5.498$  GeV $^{-2}$ , although we consider the chiral ( $m_0 = 0$ ) limit.

Figure 2 shows  $\Omega$  as a function of  $\theta$  in two cases of  $T = 250$  MeV and 300 MeV. The potential  $\Omega$  is smooth everywhere in the low  $T$  case, but not at  $\theta = (2k+1)\pi/3$  in the high  $T$  case. This result is consistent with the RW prediction [9] and lattice simulation [8] on the  $\theta$  and the  $T$  dependence of the QCD thermodynamic potential.

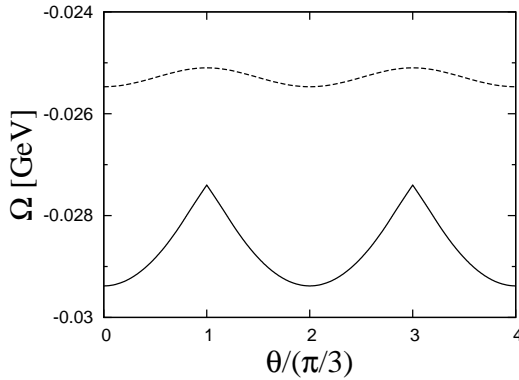


Fig. 2: Thermodynamic potential  $\Omega$  as a function of  $\theta$ . The solid line represents a result of the case of  $T = 300$  MeV, and the dashed one corresponds to that of  $T = 250$  MeV.

Figure 3 shows the real and imaginary parts of the modified Polyakov loop  $\Psi(\theta)$ . In the case of  $T = 300$  MeV, the imaginary part of  $\Psi(\theta)$  is discontinuous at  $\theta = (2k+1)\pi/3$ , while the real part of  $\Psi(\theta)$  is continuous but not smooth there. Thus, the deconfinement phase transition of first order appears at  $\theta = (2k+1)\pi/3$  in the high  $T$  region. This is precisely the RW phase transition. In the case of  $T = 250$  MeV, meanwhile, both the real and the imaginary part are smooth everywhere. All the results on the  $\theta$  and the  $T$  dependence of  $\Psi$  are consistent with the RW prediction on it and the results of lattice simulations [3, 5, 7]. The present analysis clearly shows that the transition is the first order in the imaginary part of  $\Psi(\theta)$ , while the preceding works discuss only the order of transition. Thus, the present analysis is more informative than the preceding analyses.

Figure 4 shows the chiral condensate  $\sigma$  as a function of  $\theta$ . In the case of  $T = 300$  MeV,  $\sigma$  has a cusp at each of  $\theta = (2k+1)\pi/3$ . Thus, the chiral phase transition of second order comes out at  $\theta = (2k+1)\pi/3$ . Meanwhile, in the case of  $T = 250$  MeV, there is no cusp at  $\theta = (2k+1)\pi/3$ , indicating no chiral phase transition there.

Figure 5 represents the phase diagram in the  $\theta$ - $T$  plane. The phase diagram is symmetric with respect to each of lines

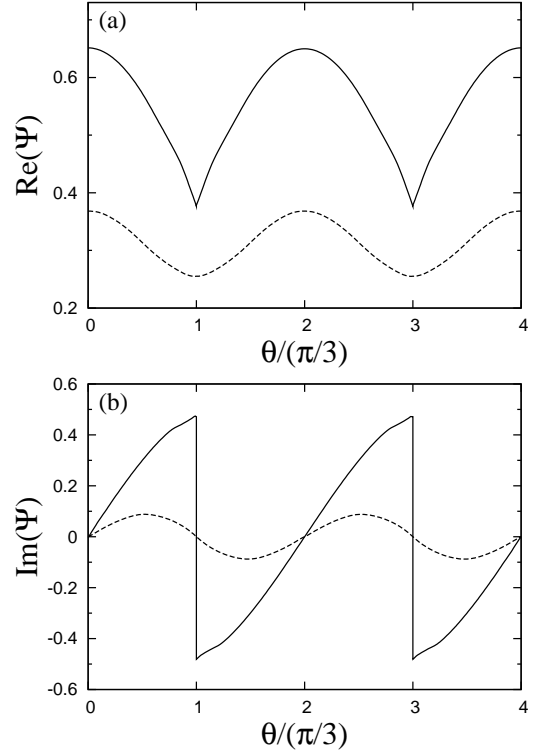


Fig. 3: The modified Polyakov loop  $\Psi(\theta)$  as a function of  $\theta$ ; (a) for the real part and (b) for the imaginary part. The definitions of lines are the same as in Fig. 2.

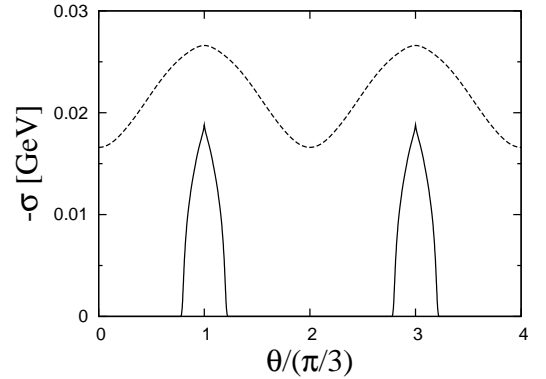


Fig. 4: Chiral condensate  $\sigma$  as a function of  $\theta$ . The definitions of lines are the same as in Fig. 2.

$\theta = k\pi/3$  for any integer  $k$ . The dashed curve between D and E represents the deconfinement phase transition of crossover, and the dot-dashed curve between C and F does the second-order chiral phase transition. For  $\theta \neq k\pi/3$ , thus, the chiral phase transition occurs at  $T$  higher than the deconfinement phase transition does. The solid vertical line starting from point E represents the RW deconfinement phase transition of first order. Both the deconfinement and the chiral phase transition occur on the line between E and F, although the decon-

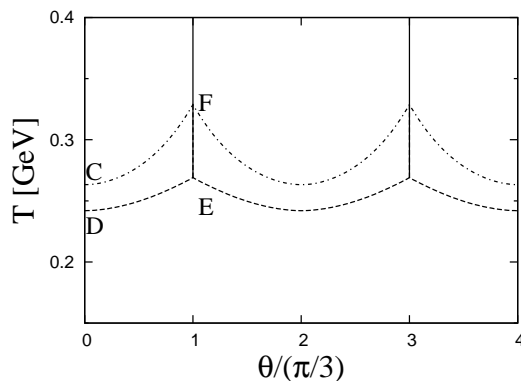


Fig. 5: The phase diagram in the  $\theta$ - $T$  plane. The solid vertical line starting from point E represents the RW deconfinement phase transition of first order. The dashed curve between D and E represents the deconfinement phase transition of crossover, and the dot-dashed curve between C and F does the second-order chiral phase transition. The second-order chiral phase transition also appears on the line between E and F.

finement phase transition is the first order and the chiral phase transition is the second order there. Point F turns out to be a bifurcation of the chiral phase transition line, and point E is the endpoint of both the deconfinement and chiral phase transitions.

Temperatures of C, D, E, F are about 261 MeV, 240 MeV, 269 MeV, 328 MeV, respectively. Thus, at  $\theta = 0$  the critical temperature of the chiral phase transition is higher by about 20 MeV than that of the deconfinement transition, and the difference is getting larger gradually as  $\theta$  increases to  $\pi/3$ . Meanwhile, the lattice simulation suggests that the two critical temperatures are almost identical not only for zero  $\theta$  but also for finite  $\theta$  [5, 6]. The difference between the two critical temperatures is reduced by a factor 3 by adding the scalar-type eight-quark interaction to the PNJL Lagrangian [20]. Further

discussion will be made in the forthcoming paper.

In summary, the phase diagram in the  $\theta$ - $T$  plane is studied with the Polyakov loop extended Nambu–Jona-Lasinio (PNJL) model. Since the PNJL model possess an extended  $\mathbb{Z}_3$  symmetry, quantities invariant under the symmetry, such as the thermodynamic potential, the chiral condensate and the modified Polyakov loop, automatically have the Roberge-Weiss periodicity that QCD does. The deconfinement phase transition of first order occurs at  $\theta = (2k + 1)\pi/3$  through the imaginary part of the modified Polyakov loop. This result is more informative than the RW prediction and the results of lattice QCD in which only the order of transition is discussed. The present model also clarifies the phase diagram of chiral transition in the chiral limit. In particular, it is of interest that there exists a bifurcation of the transition line. In this paper, our discussion is focused only on qualitative comparison with the results of lattice simulation. Quantitative comparison will be made in the forthcoming paper.

The success of the PNJL model comes from the fact that the PNJL model has the extended  $\mathbb{Z}_3$  symmetry, more precisely that the thermodynamic potential (16) is a function only of variables,  $\Psi$ ,  $\Psi^*$ ,  $e^{\pm\beta\mu_B}$  and  $\sigma$ , invariant under the extended  $\mathbb{Z}_3$  symmetry. A reliable effective theory of QCD proposed in future is expected to have the same property in its thermodynamic potential. This may be a good guiding principle to elaborate an effective theory of QCD.

### Acknowledgments

The authors thank M. Matsuzaki and T. Murase for useful discussions and suggestions. H.K. thanks M. Imachi, H. Yoneyama and M. Tachibana for useful discussions about the RW phase transition. This work has been supported in part by the Grants-in-Aid for Scientific Research (18540280) of Education, Science, Sports, and Culture of Japan.

- 
- [1] J. Kogut, M. Stone, H. W. Wyld, W. R. Gibbs, J. Shigemitsu, S. H. Shenker, and D. K. Sinclair, Phys. Rev. Lett. **50**, 393 (1983).
  - [2] J. B. Kogut and D. K. Sinclair arXiv:hep-lat/0712.2625 (2007).
  - [3] P. de Forcrand and O. Philipsen, Nucl. Phys. **B642**, 290 (2002).
  - [4] P. de Forcrand and O. Philipsen, Nucl. Phys. **B673**, 170 (2003).
  - [5] M. D’Elia and M. P. Lombardo, Phys. Rev. D **67**, 014505 (2003).
  - [6] M. D’Elia and M. P. Lombardo, Phys. Rev. D **70**, 074509 (2004).
  - [7] H. S. Chen and X. Q. Luo, Phys. Rev. **D72**, 034504 (2005).
  - [8] M. P. Lombardo, arXiv:hep-lat/0612017 (2006).
  - [9] A. Roberge and N. Weiss, Nucl. Phys. **B275**, 734 (1986).
  - [10] Y. Nambu and G. Jona-Lasinio, Phys. Rev. **122**, 345 (1961); Phys. Rev. **124**, 246 (1961).
  - [11] P. N. Meisinger, and M. C. Ogilvie, Phys. Lett. B **379**, 163 (1996).
  - [12] K. Fukushima, Phys. Lett. B **591**, 277 (2004).
  - [13] S. K. Ghosh, T. K. Mukherjee, M. G. Mustafa, and R. Ray, Phys. Rev. D **73**, 114007 (2006).
  - [14] E. Megías, E. R. Arriola, and L. L. Salcedo, Phys. Rev. D **74**, 065005 (2006).
  - [15] C. Ratti, M. A. Thaler, and W. Weise, Phys. Rev. D **73**, 014019 (2006).
  - [16] C. Ratti, S. Rößner, M. A. Thaler, and W. Weise, Eur. Phys. J. C **49**, 213 (2007).
  - [17] S. Rößner, C. Ratti, and W. Weise, Phys. Rev. D **75**, 034007 (2007).
  - [18] H. Hansen, W. M. Alberico, A. Beraudo, A. Molinari, M. Nardi, and C. Ratti, Phys. Rev. D **75**, 065004 (2007).
  - [19] C. Sasaki, B. Friman, and K. Redlich, Phys. Rev. D **75**, 074013 (2007).
  - [20] K. Kashiwa, H. Kouno, M. Matsuzaki, and M. Yahiro, arXiv:hep-ph/0710.2180 (2007).
  - [21] M. Asakawa and K. Yazaki, Nucl. Phys. **A504**, 668 (1989).
  - [22] M. Kitazawa, T. Koide, T. Kunihiro, and Y. Nemoto, Prog. Theor. Phys. **108**, 929 (2002).
  - [23] K. Kashiwa, H. Kouno, T. Sakaguchi, M. Matsuzaki, and M. Yahiro, Phys. Lett. B **647**, 446 (2007).

- [24] K. Kashiwa, M. Matsuzaki, H. Kouno, and M. Yahiro, Phys. Lett. B **657**, 143 (2007).
- [25] G. Boyd, J. Engels, F. Karsch, E. Laermann, C. Legeland, M. Lütgemeier, and B. Petersson, Nucl. Phys. **B469**, 419 (1996).
- [26] O. Kaczmarek, F. Karsch, P. Petreczky, and F. Zantow, Phys. Lett. B **543**, 41 (2002).